S. Saitta, R. Luciano, R. Vescovini, N. Fantuzzi, F. Fabbrocino
Optimization of a Radial Point Interpolation Meshless Strategy for Strain Gradient Nanoplates
Engineering Analysis with Boundary Elements, Vol. 140, 2022, p. 70-78
doi:10.1016/j.enganabound.2022.03.026

Optimization of a Radial Point Interpolation Meshless Strategy for Strain Gradient Nanoplates

Serena Saitta[a], Raimondo Luciano[b], Riccardo Vescovini[c], Nicholas Fantuzzi*[d], Francesco Fabbrocino[a]

[a]*Department of Engineering, Telematic University Pegaso, Centro Direzionale Isola F2, Napoli, 80143, Italy*
[b]*Department of Engineering, Parthenope University, Centro Direzionale ISOLA C4, Napoli, 80133, Italy*
[c]*Department of Aerospace Science and Technology, Politecnico di Milano, Via La Masa, 34, Milano, 20156, Italy*
[d]*Department of Civil, Chemical, Environmental, and Materials Engineering, University of Bologna, Viale del Risorgimento, Bologna, 40136, Italy*

Abstract

A parameter optimization of the Radial Point Interpolation meshless Method (RPIM) is presented in this work for solving the static bending analysis of Kirchhoff nanoplates which include the second order strain gradient theory. Optimization in meshless strategies is often required since shape parameters, of the Radial Basis Functions (RBFs) used, might vary due to different plate geometries and various boundary conditions are studied. Due to the introduction of a second strain gradient theory within Kirchhoff plate framework, to approximate the bending degrees of freedom, a Hermite RPIM is used. The results of the static analysis are compared with the solutions available in the literature and good agreement among all presented results as well as convergence behavior is shown.

Keywords: Optimization method, Radial Point Interpolation Method, Strain gradient theory, Mesh less method, Genetic algorithm

*Corresponding author, nicholas.fantuzzi@unibo.it

1. Introduction

In recent years, the field of research on the topic of mesh free methods has proven do be dynamic and in continuous evolution. The idea of the methods is to discretize the continuum domain using a set of randomly scattered nodes rather than discretize it by means of a mesh. The absence of a mesh allows to spare a significant amount of time during the analysis and introduces a huge degree of flexibility in terms of introducing or removing nodes from the domain. However, if the problem is studied in its weak formulation, a mesh has to be introduced for the sole purpose of integrals numerical evaluation.

Mesh free methods have been widely applied to classical structural mechanics analysis [1]. A number of methods exist each one characterised by a different procedure used to calculate the shape functions [1, 2]. Among them, the Radial Point Interpolation Method (RPIM) can be convenient since it possesses the Kronecker delta function property which allows to impose the essential boundary conditions in the same way as in conventional FEM [3, 4, 5]. In its Hermite formulation, it also allows to consider additional degrees of freedom in the description to better represent the behaviour of the solid [6].

On the other hand, researcher's attention is growing towards nano structural components. Both MEMS (Micro-Electro-Mechanical-Systems) and NEMS (Nano-Electro-Mechanical-Systems) require the employment of nano structures to which classical theory don't apply [7, 8, 9, 10, 11]. In fact, the mechanical behaviour of micro and nano structures is strongly affected by the mechanic of the material and by the long range interactions between particles [12, 13]. These aspects, while weak at macroscale, become significant on microscale. Classical theories are not able to account for these microscopic effect. Nonlocal theories, instead, have been widely applied for both the static [14, 15] and dynamic [9, 16, 17] analysis of structures in which nonlocal effects are not negligible.

Bending analysis of micro-sized beams based on the Bernoulli-Euler beam theory has been studied within the modified strain gradient elasticity and modified couple stress theories. The influence of size effect and additional material parameters on the static response of micro-sized beams in bending has also been studied. The bending values obtained by these higher-order elasticity theories have a significant difference with those calculated by the classical elasticity theory [13]. Faghidian et al. [18] proposed a mixture stress gradient theory of elasticity conceived via consistent unification of the

classical elasticity theory and the stress gradient theory within a stationary variational framework. In particular a boundary-value problem associated with a functionally graded nano-bar is rigorously formulated. Static bending response of single-walled carbon nanotubes (SWCNTs) embedded in an elastic medium has also been investigated on the basis of higher-order shear deformation microbeam models in conjunction with modified strain gradient theory. The results obtained show that the bending behavior of SWCNTs is dependent on the small-size, stiffness of the elastic foundation and also effects of shear deformation, especially for smaller slenderness ratios [19]. Large-amplitude nonlinear vibration response of symmetric porous functionally graded (FG) nanobeams carrying several fullerenes has been analyzed in [20] where the influence of various porosity distributions as well as position and mass of fullerenes on the nonlinear vibrational behaviour is particularly studied. Piezoelectric effect of porous nanobeams has been analysis using a meshless DQ method for vibrations in [21].

One of the most used theory in the analysis of nanostructures is Eringen's nonlocal elasticity theory which can be improved by adding additional parameters thus obtaining an enhanced Eringen differential model. Bending of nano/micro beams under concentrated and distributed loads and subjected to various types of boundary conditions have been investigated using such differential model [22].

A number of numerical finite element implementation of the nonlocal strain gradient theory applied to thin laminated composite nanoplates using Kirchhoff theory (known as Classical Laminated Plate Theory or CLPT). Hermite interpolation functions are used to approximate membrane and bending degrees of freedom according to the conforming and nonconforming approaches [23, 24, 25, 26].

To the best of the authors' knowledge, mesh free Methods and nonlocal theories have not yet been used together to solve structural mechanics problems. The challenge of the present work is to implement a RPIM to solve the static bending problem of nanoplates modelled via negative strain gradient theory and to search for an optimal combination of shape parameter to obtain the most accurate results possible [27].

The paper is organized as follows. The present introduction precedes a section dedicated to theoretical notions on thin isotropic Kirchhoff plates and strain gradient formulation. Which is then followed by a detailed explanation of the Radial Point Interpolation Method, shape functions construction and numerical implementation. Within this context, a section on the importance

of the nondimensional parameters is introduced and the optimization procedure is widely explained. The last section presents the numerical results and convergence plots that validate and compare the present analysis against the analytical solutions available in the literature. Finally, a conclusion sections summarize the previous topics and closes the work.

2. Isotropic thin plate model

The behaviour of a thin isotropic plate subjected to a uniformly distributed transverse load is studied. The plate has dimensions $a \times b$ being a the length along the x-axis and b along the y-axis. The thickness h is considered uniform along the whole plate and the transverse static load of magnitude q_z is applied in the z direction.

2.1. Kinematics

According to Kirchhoff flexural plate theory [28], the displacements u, v and w along the x, y and z axis respectively, are written as a function of the degrees of freedom on the mid section of the plate. For isotropic plates in bending the only degree of freedom is the transverse displacement w of the mid-point $(x, y, 0)$:

$$u(x, y, z) = -z\frac{\partial w(x, y, z)}{\partial x} \tag{1}$$

$$v(x, y, z) = -z\frac{\partial w(x, y, z)}{\partial y} \tag{2}$$

$$w(x, y, z) = w(x, y, z) \tag{3}$$

Subsequently, the strains are written as:

$$\boldsymbol{\varepsilon} = z\mathbb{D}w(x, y) \tag{4}$$

where $\boldsymbol{\varepsilon} = \begin{Bmatrix} \varepsilon_{xx} & \varepsilon_{yy} & \gamma_{xy} \end{Bmatrix}^\top$ is the three dimensional strain vector and $\mathbb{D}$ is the differential operator defined as:

$$\mathbb{D} = \begin{bmatrix} -\frac{\partial^2}{\partial x^2} & -\frac{\partial^2}{\partial y^2} & -2\frac{\partial^2}{\partial xy} \end{bmatrix}^\top \tag{5}$$

2.2. Strain gradient theory

Under plane stress assumptions, the stress-strain relationship is expressed through the constitutive law. The negative strain gradient theory enters directly the constitutive law introducing a nonlocal parameter ℓ:

$$\boldsymbol{\sigma} = (1 - \ell^2 \Delta^2)\bar{\mathbf{Q}}\boldsymbol{\varepsilon} \tag{6}$$

where $\boldsymbol{\sigma} = \{\sigma_{xx} \quad \sigma_{yy} \quad \tau_{xy}\}^\top$, $\Delta^2 = \partial^2/\partial y^2 + \partial^2/\partial x^2$ denotes the Laplacian operator and $\bar{\mathbf{Q}}$ is the matrix of reduced material constants.

2.3. Equations of motion

The equations of motion of the problem are derived from the principle of virtual work (PVW):

$$\int_A \left(\delta\boldsymbol{\varepsilon}^\top \boldsymbol{\sigma} - \delta w(x,y) q_z \right) dA = 0 \tag{7}$$

being A the plate surface and q_z is transverse distributed load applied to the plate.

Recalling Equation (4) and the constitutive law as given in Equation (6), it can be rewritten as follows:

$$\int_A \left\{ \delta w^\top \left[\mathbb{D}^{(b)\top} \mathbf{D} \mathbb{D}^{(b)} + \ell^2 \left(\mathbb{D}^{(b)\top}_{,x} \mathbf{D} \mathbb{D}^{(b)}_{,x} + \mathbb{D}^{(b)\top}_{,y} \mathbf{D} \mathbb{D}^{(b)}_{,y} \right) \right] w + \delta w^\top \mathbf{q}_z \right\} dA = 0 \tag{8}$$

where

$$\mathbb{D}_{,x} = -\frac{\partial}{\partial x}\mathbb{D} \qquad \mathbb{D}_{,y} = -\frac{\partial}{\partial y}\mathbb{D} \tag{9}$$

In the previous equation, $\mathbf{D}$ is the material constant matrix expressed as:

$$\mathbf{D} = \frac{Eh^3}{12(1-\nu^2)} \begin{bmatrix} 1 & \nu & 0 \\ \nu & 1 & 0 \\ 0 & 0 & \frac{1-\nu}{2} \end{bmatrix} \tag{10}$$

for plane strain problems. Here, E is the Young's modulus and ν is the Poisson's ratio.

3. Mesh free Model

In the present work the numerical analysis makes use of a meshfree approach termed Radial Point interpolation Method (RPIM). Thus, on the one hand no mesh is required to discretize the problem. The domain and the boundaries are simply represented by a regularly distributed set of nodes. On the other hand, the RPIM posses the Kronecker delta function property which allows to impose the essential boundary conditions in the same way as in conventional FEM.

Differently from FEM, however, the shape functions built with the RPIM do not already embed all the necessary degrees of freedom at the node. This poses an issue for the imposition of the boundary conditions. In the case of a Kirchhoff plate, the only degree of freedom is the transverse deflection w. In this work, however, due to the higher order derivatives introduced by the strain gradient formulation, both the deflection w and its first derivatives w_x and w_y are taken as variables. Any higher-order derivative can be simply obtained by derivation. Therefore, it is more convenient, if not necessary, to use the Hermite-RPIM rather than the classical formulation [6].

The approximation of the field function $w(x, y)$ is written as a linear combination of radial basis functions (RBF) and their derivatives at all the n nodes falling within a local domain called support domain:

$$\begin{aligned} w(x,y) &= \sum_{i=1}^{n} R_i(x,y)a_i + \sum_{i=1}^{n} R_{i,x}(x,y)a_i^x + \sum_{i=1}^{n} R_{i,y}(x,y)a_i^y \\ &= \mathbf{R}^\top(\mathbf{x})\mathbf{a} + \mathbf{R}_{,x}^\top(\mathbf{x})\mathbf{a}^x + \mathbf{R}_{,y}^\top(\mathbf{x})\mathbf{a}^y \end{aligned} \tag{11}$$

where $R_i(x, y)$, $R_{i,x}(x, y)$ and $R_{i,y}$ are the RBF and its derivatives and a_i, a_i^x and a_i^y the corresponding unknown vectors of coefficients.

There are many RBFs to choose from. In this work, the multi-quadrics (MQ) RBF [30, 29] is used in the form:

$$R_i(x) = [(x - x_i)^2 + (y - y_i)^2 + C^2]^q \tag{12}$$

where q and $C = \alpha_C d_c$ are the shape parameters. Both q and α_C nondimensional parameters require some tuning to ensure numerical accuracy of the results.

The derivative of the field function $w(x, y)$ is considered equal to the derivative of its approximation function. The vector of coefficients in Equation (11) are obtained by enforcing the field function and its derivative to be

satisfied at all the n nodes enclosed in the support domain. This leads to a system of $3n$ linear equations [31] written in matrix form as:

$$\mathbf{W} = \begin{Bmatrix} \mathbf{w} \\ \mathbf{w}_{,x} \\ \mathbf{w}_{,y} \end{Bmatrix} = \begin{bmatrix} \mathbf{R} & \mathbf{R}_{,x} & \mathbf{R}_{,y} \\ \mathbf{R}_{,x} & \mathbf{R}_{,xx} & \mathbf{R}_{,xy} \\ \mathbf{R}_{,y} & \mathbf{R}_{,xy} & \mathbf{R}_{,yy} \end{bmatrix} \begin{bmatrix} \mathbf{a} \\ \mathbf{a}^x \\ \mathbf{a}^y \end{bmatrix} = \mathbf{G}\mathbf{a} \tag{13}$$

where $\mathbf{w}$, $\mathbf{w}_{,x}$ and $\mathbf{w}_{,y}$ are vectors of function values in the form:

$$\mathbf{w} = \begin{bmatrix} w_1 & w_2 \dots w_n \end{bmatrix}^\top \tag{14}$$

$$\mathbf{w}_{,x} = \begin{bmatrix} w_{1,x} & w_{2,x} \dots w_{n,x} \end{bmatrix}^\top \tag{15}$$

$$\mathbf{w}_{,y} = \begin{bmatrix} w_{1,y} & w_{2,y} \dots w_{n,y} \end{bmatrix}^\top \tag{16}$$

Solving Equation (13) and substituting into Equation (11) we obtain:

$$\begin{aligned} w(x,y) &= \begin{bmatrix} \mathbf{R}^\top & \mathbf{R}_{,x}^\top & \mathbf{R}_{,y}^\top \end{bmatrix} \begin{bmatrix} \mathbf{a} \\ \mathbf{a}^x \\ \mathbf{a}^y \end{bmatrix} \\ &= \begin{bmatrix} \mathbf{R}^\top & \mathbf{R}_{,x}^\top & \mathbf{R}_{,y}^\top \end{bmatrix} \mathbf{G}^{-1}\mathbf{W} \end{aligned} \tag{17}$$

The Hermite-RPIM shape functions are then written as:

$$\begin{aligned} \mathbf{\Phi}^\top(\mathbf{x}) &= \begin{bmatrix} \mathbf{R}^\top & \mathbf{R}_{,x}^\top & \mathbf{R}_{,y}^\top \end{bmatrix} \mathbf{G}^{-1} = \begin{bmatrix} \boldsymbol{\varphi} & \boldsymbol{\varphi}^x & \boldsymbol{\varphi}^y \end{bmatrix} \\ &= \begin{bmatrix} \varphi_1 \dots \varphi_i \dots \varphi_n & \varphi_1^x \dots \varphi_i^x \dots \varphi_n^x & \varphi_1^y \dots \varphi_i^y \dots \varphi_n^y \end{bmatrix} \end{aligned} \tag{18}$$

Once the shape functions have been obtained, the procedure is the same as in conventional FEM. The approximation is directly introduced in the weak form of the equation of motion:

$$\int_A \delta\mathbf{W} \left[\mathbb{D}^{(b)}\mathbf{\Phi}^\top \mathbf{D} \mathbb{D}^{(b)}\mathbf{\Phi} + \ell^2 (\mathbb{D}_{,x}^{(b)}\mathbf{\Phi}^\top \mathbf{D} \mathbb{D}_{,x}^{(b)}\mathbf{\Phi} + \mathbb{D}_{,y}^{(b)}\mathbf{\Phi}^\top \mathbf{D} \mathbb{D}_{,y}^{(b)}\mathbf{\Phi}) + \mathbf{\Phi}^\top q_z \right] dA = 0 \tag{19}$$

Equation (19) can be written for every node in the domain. The assemble of all contributions yields the usual, well known equation of motion:

$$\mathbf{K}\mathbf{W} = \mathbf{F} \tag{20}$$

The stiffness matrix of the previous equation is the summation of two terms:

$$\mathbf{K} = \mathbf{K_c} + \mathbf{K_{sg}} \tag{21}$$

where:

$$\mathbf{K}_{\mathbf{c}i} = \int_A \mathbb{B}_i^\top \mathbf{D} \mathbb{B}_i dA \tag{22}$$

is the classical component of the stiffness matrix for the i-th node, and

$$\mathbf{K}_{\mathbf{sg}_i} = \int_A \ell^2 \left(\mathbb{B}_{,x_i}^\top \mathbf{D} \mathbb{B}_{,x_i} + \mathbb{B}_{,y_i}^\top \mathbf{D} \mathbb{B}_{,y_i} \right) dA \tag{23}$$

is the corresponding strain gradient component. Moreover, the three matrices of shape functions derivative are expressed as:

$$\mathbb{B}_i = \mathbb{D} \mathbf{\Phi}_i \qquad \mathbb{B}_{,x_i} = \mathbb{D}_{,x} \mathbf{\Phi}_i \qquad \mathbb{B}_{,y_i} = \mathbb{D}_{,y} \mathbf{\Phi}_i \tag{24}$$

Following the same procedure, the load vector for the i-th node is writte as:

$$\mathbf{F} = \int_A \mathbf{\Phi}_i q_z \; dA \tag{25}$$

4. Influence of parameters

The MQ radial basis function [32, 33] depends on the two nondimensional parameters C and q, as shown in Equation (12). It has been widely shown [1] how the tuning of the shape parameters affects the numerical results of the analysis. The tuning is not completely arbitrary since the admissible values of these parameter are bounded by limits provided in literature. Still, even if some numbers emerged which give better results, it is not always guaranteed that they may give good results for every geometry or boundary condition considered.

Moreover, the construction of shape functions in meshfree methods is performed using only the information of nodes falling inside a local domain called support domain. The size of which can be expressed as:

$$d_s = \alpha_s d_c \tag{26}$$

where d_c is the average nodal spacing $d_c = \sqrt{\Delta x^2 + \Delta y^2}$ and α_s is another nondimensional parameter to be tuned.

Overall, there are three parameters that affect the quality of the results of the analysis. In this case, in particular, the use of the strain gradient theory to model the plate complicates things due to the need of computing higher order derivatives which contributes to the reduction of the accuracy of the results.

4.1. Optimization

In this work, an optimal combination of the three parameters is sought to assess whether a certain combination that grants good results exists. The analysis is performed by seeking the best possible results for plates with different geometries and considering different kind of boundary conditions. More specifically, each geometry is optimised independently while seeking one single combination of the three nondimensional parameters which grants the best results for all the boundary conditions considered.

The solution of merely the analysis is a vector containing the nondimensional mid deflections of the current plate expressed as:

$$\bar{w} = \frac{1000 w_{max} D}{q_z a^4} \tag{27}$$

where w_{max} is the maximum deflection, q_z is the magnitude of the external load (considered uniform) and D is the bending rigidity $D = Eh^3/12(1-\nu^2)$. Each entry of the vector corresponds to the deflection relative to a different boundary condition.

Similarly, a vector of percentage error is computed in the same way. Each entry refers to a different boundary condition and is defined as:

$$err_{\%} = 100 \frac{|w_e - \bar{w}|}{w_e} \tag{28}$$

where $\bar{w}$ is defined in Equation (27) and w_e is the exact solution taken from Ref [15]. The object that is optimized is the norm of such error vector and the optimization itself is performed by means of the Genetic Algorithm MATLAB Toolbox.

4.2. The Genetic Algorithm

The problem here described is a constrained optimization problem. The aim is to find an optimal combination of nondimensional parameters which grants the minimum percentage error between the numerical and analytical solution. The constraint comes by the limits on the values that the parameters can assume. As stated in [1], these ranges are given as:

$$1 \leq \alpha_c \leq 3 \tag{29}$$

$$-3.5 \leq q \leq 3.5 \tag{30}$$

$$1.8 \leq \alpha_s \leq 3 \tag{31}$$

The Genetic Algorithm (GA) allows to solve both constrained and unconstrained optimization problems using a procedure which emulates biological evolution and the natural selection process it is based on. The function to optimize is called fitness function and, in the case described in this work, it is given by the program performing the static analysis of the nanoplates considered, which takes into account different geometries and boundary conditions.

The GA is an iterative process which begins with the creation of an initial population. In the present paper, this is given by a first initial guess of the three dimensionless parameters α_c, q and α_s. Then, the algorithm generates a sequence of new populations by selecting individuals in the current generation to create the next one. This procedure is made by following some intermediate steps.

Each member of the current population is scored according to its fitness value, called raw fitness score. The latter is converted in a more usable value called expectation value. According to their expectation, some members of the current population are chosen to be parents. The ones with the lowest fitness value are chosen as elite and are certainly passed on to the next generation. The parents selected with this process, produce children in two ways. Either a single parent undergoes a random change, called a mutation, or two parents are combined in a process called crossover. The current generation is then replaced by these new children [34]. The GA stops when the stopping criterion is met.

Concerning the constraints, [1, 2] state that q can not assume an integer value. Since the Genetic Algorithm does not contemplate any such kind of constraints, a manual check is introduced directly inside the fitness function. Using an if conditional statement, every time an integer value of q is chosen in a generation, an additional 0.01 is added to that value so that the input to the fitness function never contains an integer q parameter.

5. Results and discussion

As aforementioned, different kinds of boundary conditions are accounted for. Table 1 shows the constraints which are used either as stated or arranged in different combinations. More specifically, five different boundary conditions are considered: SSSS, CCCC, SCSC, SFSF, SCSF. Here the first and third edges represent $x = 0, a$ while the second and fourth $y = 0, b$.

It can be observed that the simultaneous optimization of plates under different kinds of boundary conditions makes the process of searching for the best solution harder than it would be if only one type of constraint would have been considered. Nevertheless, the results show good convergence with the analytical solution. Numerical results tend to degrade as the value of the nonlocal parameter ℓ increases. This trend may be explained by the relative weight that higher order derivatives have as the nonlocal parameter value changes. In fact, the strain gradient theory requires the computation of higher order derivatives of the RBF of the meshfree method, which introduces numerical errors. As the value of ℓ increases, the weight of the higher order derivatives in the computations increases as well, causing the degradation of accuracy of the results of the analysis.

Table 1: Basic Essential boundary conditions.

BCs	$x = 0, a$	$y = 0, b$
Supported	$w = \frac{\partial w}{\partial y} = 0$	$w = \frac{\partial w}{\partial x} = 0$
Clamped	$w = \frac{\partial w}{\partial x} = \frac{\partial w}{\partial y} = 0$	$w = \frac{\partial w}{\partial x} = \frac{\partial w}{\partial y} = 0$
Free	–	–

The analysis is performed considering 15×15 regularly distributed nodes to represent the domain. Moreover, 3×3 Gauss points are used to evaluate the integrals shown in Equations (22), (23) and (25).

The results are shown in Tables 2 to 5.

A graphical representation of the variation of the behaviour with the number of nodes is also presented in Figures 1 to 4. The nondimensional parameters α_C, q and α_s are obtained with the optimization procedure described in Section 4.2 and their value changes as the number of nodes varies.

6. Conclusion

The analysis of isotropic rectangular nanoplates modelled according to the second order strain gradient theory is presented. The aim was to apply a meshfree RPIM to strain gradient Kirchhoff nanoplates and find an optimal combination of non dimensional parameters via an optimization procedure. The thin plates are characterised by different aspect ratios b/a and subjected to different constraints: SSSS, CCCC, SCSC, SFSF, SCSF. The bending analysis is performed as an external distributed transverse load is applied

Table 2: Non dimensional values of $\bar{w}$ for $b/a = 0.5$ obtained for $\alpha_C = 1$, $q = 1.01$ and $\alpha_s = 2.3$

	ℓ (nm)	Analytical	Present	Error (%)
SSSS	0	0.6330	0.6321	0.1422
	0.2	0.6218	0.6214	0.0643
	0.5	0.5680	0.5773	1.6373
	1	0.4316	0.4787	10.9129
CCCC	0	0.1583	0.1597	0.8844
	0.2	0.1477	0.1482	0.3385
	0.5	0.1109	0.1108	0.0902
	1	0.0590	0.0586	0.6780
SCSC	0	0.1632	0.1645	0.7966
	0.2	0.1523	0.1528	0.3283
	0.5	0.1146	0.1145	0.0873
	1	0.0612	0.0608	0.6536
SFSF	0	14.6446	14.4269	1.4866
	0.2	14.5814	14.3486	1.5966
	0.5	14.2561	13.9893	1.8715
	1	13.2005	13.0033	1.4939
SCSF	0	3.6392	3.6332	0.1649
	0.2	3.5976	3.5830	0.4058
	0.5	3.4102	3.3764	0.9911
	1	2.9111	2.8330	2.6828

Table 3: Non dimensional values of $\bar{w}$ for $b/a = 1$ obtained for $\alpha_C = 2.25$, $q = 0.1$ and $\alpha_s = 2.2$

	ℓ (nm)	Analytical	Present	Error (%)
SSSS	0	4.0624	4.0481	0.3520
	0.2	4.0330	4.0197	0.3298
	0.5	3.8844	3.8824	0.0515
	1	3.4231	3.4794	1.5132
CCCC	0	1.2653	1.2688	0.2766
	0.2	1.2333	1.2357	0.3405
	0.5	1.0979	1.1061	0.7469
	1	0.7946	0.8101	1.9507
SCSC	0	1.9171	1.9174	0.0156
	0.2	1.8783	1.8797	0.0745
	0.5	1.7093	1.7169	0.4446
	1	1.3040	1.3255	1.6488
SFSF	0	15.0113	14.9837	0.1839
	0.2	14.9470	14.9181	0.1933
	0.5	14.6165	14.6244	0.0540
	1	13.5415	13.8130	1.9778
SCSF	0	11.2359	11.2265	0.0837
	0.2	11.1703	11.1589	0.1021
	0.5	10.8454	10.8431	0.0212
	1	9.8416	9.9234	0.8312

Table 4: Non dimensional values of $\bar{w}$ for $b/a = 2$ obtained for $\alpha_C = 1.45$, $q = 0.4$ and $\alpha_s = 2.2$

	ℓ (nm)	Analytical	Present	Error (%)
SSSS	0	10.1287	10.0658	0.6210
	0.2	10.0833	10.0201	0.6268
	0.5	9.8502	9.8101	0.4071
	1	9.0886	9.1925	1.1432
CCCC	0	2.5330	2.5393	0.2487
	0.2	2.4861	2.4933	0.2896
	0.5	2.2799	2.2983	0.8071
	1	1.7741	1.8168	2.4069
SCSC	0	8.4450	8.4164	0.3387
	0.2	8.3887	8.3573	0.3743
	0.5	8.1145	8.0858	0.3537
	1	7.2820	7.3155	0.4600
SFSF	0	15.2022	15.2614	0.3894
	0.2	15.1373	15.1641	0.1770
	0.5	14.8040	14.7387	0.4411
	1	13.7211	13.6624	0.4278
SCSF	0	14.9491	15.0169	0.4535
	0.2	14.8838	14.9188	0.2352
	0.5	14.5493	14.4889	0.4151
	1	13.4658	13.3879	0.5785

Table 5: Non dimensional values of $\bar{w}$ for $b/a = 3$ obtained for $\alpha_C = 1.5$, $q = -0.25$ and $\alpha_s = 2.5$

	ℓ (nm)	Analytical	Present	Error (%)
SSSS	0	12.2328	12.3211	0.7218
	0.2	12.1839	12.2706	0.7116
	0.5	11.9324	12.0541	1.0199
	1	11.1046	11.4793	3.3743
CCCC	0	2.6172	2.6660	1.8646
	0.2	2.5706	2.9041	1.3032
	0.5	2.3639	2.3893	1.0745
	1	1.8518	1.8687	0.9126
SCSC	0	11.6813	11.7718	0.7747
	0.2	11.6286	11.7172	0.7619
	0.5	11.3623	11.4797	1.0332
	1	10.5039	10.8382	3.1826
SFSF	0	15.2181	15.5101	1.9188
	0.2	15.1532	15.3223	1.1159
	0.5	14.8196	14.6152	1.3793
	1	13.7361	13.0677	4.8660
SCSF	0	15.2035	15.4984	1.9397
	0.2	15.1385	15.3109	1.1388
	0.5	14.8049	14.6037	1.3590
	1	13.7212	13.0548	4.8567

to the plate. According to the current state of the art, an implementation of RPIM with higher-order partial differential equations has never been presented in the literature. The paper provides a detailed explanation of the RPIM implementation together with theoretical notions presented in matrix form. A description of the working principle of the MATLAB Genetic Algorithm, used to perform the optimization, is also provided. Numerical convergence with the analytical results achieved in recent literature was studied as well as numerical convergence as the nodal density varies.

References

[1] G.R. Liu. *Mesh Free Methods: Moving beyond the Finite Element Method, Second Edition (2nd ed.)* CRC Press, 2009. DOI: https://doi.org/10.1201/9781420082104.

[2] Gui-Rong Liu and Yuan-Tong Gu. *An introduction to meshfree methods and their programming*. Springer Science & Business Media, 2005.

[3] JG Wang and GRs Liu. "A point interpolation meshless method based on radial basis functions". In: *International Journal for Numerical Methods in Engineering* 54.11 (2002), pp. 1623–1648.

[4] Gui-Rong Liu et al. "A meshfree radial point interpolation method (RPIM) for three-dimensional solids". In: *Computational Mechanics* 36.6 (2005), pp. 421–430.

[5] Yan Li et al. "A node-based smoothed radial point interpolation method with linear strain fields for vibration analysis of solids". In: *Engineering Analysis with Boundary Elements* 114 (2020), pp. 8–22.

[6] Xiangyang Cui, Guirong Liu, and Guangyao Li. "A smoothed Hermite radial point interpolation method for thin plate analysis". In: *Archive of Applied Mechanics* 81.1 (2011), pp. 1–18.

[7] Bekir Akgöz and Ömer Civalek. "Bending analysis of FG microbeams resting on Winkler elastic foundation via strain gradient elasticity". In: *Composite Structures* 134 (2015), pp. 294–301.

[8] Raffaele Barretta et al. "A gradient Eringen model for functionally graded nanorods". In: *Composite Structures* 131 (2015), pp. 1124–1131.

[9] Andrea Apuzzo et al. "Free vibrations of Bernoulli-Euler nano-beams by the stress-driven nonlocal integral model". In: *Composites Part B: Engineering* 123 (2017), pp. 105–111.

[10] Bekir Akgöz and Ömer Civalek. "A microstructure-dependent sinusoidal plate model based on the strain gradient elasticity theory". In: *Acta Mechanica* 226.7 (2015), pp. 2277–2294.

[11] Piotr Jankowski et al. "On the piezoelectric effect on stability of symmetric FGM porous nanobeams". In: *Composite Structures* 267 (2021), p. 113880. ISSN: 0263-8223. DOI: https://doi.org/10.1016/j.compstruct.2021.113880. URL: https://www.sciencedirect.com/science/article/pii/S0263822321003408.

[12] Bishweshwar Babu and BP Patel. "A new computationally efficient finite element formulation for nanoplates using second-order strain gradient Kirchhoff's plate theory". In: *Composites Part B: Engineering* 168 (2019), pp. 302–311.

[13] Bekir Akgöz and Ömer Civalek. "Analysis of micro-sized beams for various boundary conditions based on the strain gradient elasticity theory". In: *Archive of Applied Mechanics* 82.3 (2012), pp. 423–443.

[14] Raffaele Barretta, Raimondo Luciano, and Francesco Marotti de Sciarra. "A fully gradient model for Euler-Bernoulli nanobeams". In: *Mathematical Problems in Engineering* 2015 (2015).

[15] Bishweshwar Babu and BP Patel. "Analytical solution for strain gradient elastic Kirchhoff rectangular plates under transverse static loading". In: *European Journal of Mechanics-A/Solids* 73 (2019), pp. 101–111.

[16] Andrea Apuzzo et al. "A closed-form model for torsion of nanobeams with an enhanced nonlocal formulation". In: *Composites Part B: Engineering* 108 (2017), pp. 315–324.

[17] F Cornacchia et al. "Analytical solution of cross- and angle-ply nano plates with strain gradient theory for linear vibrations and buckling". In: *Mechanics of Advanced Materials and Structures* 28.12 (2021), pp. 1201–1215.

[18] S. Ali Faghidian et al. "On the analytical and meshless numerical approaches to mixture stress gradient functionally graded nano-bar in tension". In: *Engineering Analysis with Boundary Elements* 134 (2022), pp. 571–580. ISSN: 0955-7997. DOI: https://doi.org/10.1016/j.enganabound.2021.11.010. URL: https://www.sciencedirect.com/science/article/pii/S0955799721003271.

[19] Bekir Akgöz and Ömer Civalek. "Bending analysis of embedded carbon nanotubes resting on an elastic foundation using strain gradient theory". In: *Acta Astronautica* 119 (2016), pp. 1–12.

[20] Krzysztof Kamil Żur et al. "On the nonlinear dynamics of porous composite nanobeams connected with fullerenes". In: *Composite Structures* 274 (2021), p. 114356. ISSN: 0263-8223. DOI: https://doi.org/10.1016/j.compstruct.2021.114356. URL: https://www.sciencedirect.com/science/article/pii/S0263822321008187.

[21] Piotr Jankowski, Krzysztof Kamil Żur, and Ali Farajpour. "Analytical and meshless DQM approaches to free vibration analysis of symmetric FGM porous nanobeams with piezoelectric effect". In: *Engineering Analysis with Boundary Elements* 136 (2022), pp. 266–289. ISSN: 0955-7997. DOI: https://doi.org/10.1016/j.enganabound.2022.01.007. URL: https://www.sciencedirect.com/science/article/pii/S0955799722000078.

[22] Çiğdem Demir and Ömer Civalek. "On the analysis of microbeams". In: *International Journal of Engineering Science* 121 (2017), pp. 14–33.

[23] M Bacciocchi, N Fantuzzi, and AJM Ferreira. "Conforming and non-conforming laminated finite element Kirchhoff nanoplates in bending using strain gradient theory". In: *Computers & Structures* 239 (2020), p. 106322.

[24] Michele Bacciocchi et al. "Linear eigenvalue analysis of laminated thin plates including the strain gradient effect by means of conforming and nonconforming rectangular finite elements". In: *Computers & Structures* 257 (2021), p. 106676.

[25] Giovanni Tocci Monaco et al. "Trigonometric solution for the bending analysis of magneto-electro-elastic strain gradient nonlocal nanoplates in hygro-thermal environment". In: *Mathematics* 9.5 (2021), p. 567.

[26] Giovanni Tocci Monaco et al. "Critical temperatures for vibrations and buckling of magneto-electro-elastic nonlocal strain gradient plates". In: *Nanomaterials* 11.1 (2021), p. 87.

[27] S. Ali Faghidian, Krzysztof Kamil Żur, and J.N. Reddy. "A mixed variational framework for higher-order unified gradient elasticity". In: *International Journal of Engineering Science* 170 (2022), p. 103603. ISSN: 0020-7225. DOI: https://doi.org/10.1016/j.ijengsci.2021.103603. URL: https://www.sciencedirect.com/science/article/pii/S0020722521001439.

[28] S. Woinowsky-Krieger S. P. Timoshenko. *Theory of Plates and Shells*. McGraw-Hill, 1959.

[29] A.J.M. Ferreira, C.M.C. Roque, and R.M.N. Jorge. "Analysis of composite plates by trigonometric shear deformation theory and multiquadrics". In: *Computers & Structures* 83.27 (2005), pp. 2225–2237.

[30] A. J. M. Ferreira. "Analysis of Composite Plates Using a Layerwise Theory and Multiquadrics Discretization". In: *Mechanics of Advanced Materials and Structures* 12.2 (2005), pp. 99–112.

[31] Francesco Fabbrocino et al. "Meshless Computational Strategy for Higher Order Strain Gradient Plate Models". In: *Mathematical and Computational Applications* 27.2 (2022).

[32] A.J.M. Ferreira. "A formulation of the multiquadric radial basis function method for the analysis of laminated composite plates". In: *Composite Structures* 59.3 (2003), pp. 385–392.

[33] A.J.M. Ferreira et al. "Static deformations and vibration analysis of composite and sandwich plates using a layerwise theory and multiquadrics discretizations". In: *Engineering Analysis with Boundary Elements* 29.12 (2005), pp. 1104–1114.

[34] Matworks. *How the Genetic Algorithm Works*.

[35] Y.T. Gu and G.R. Liu. "A local point interpolation method for static and dynamic analysis of thin beams". In: *Computer Methods in Applied Mechanics and Engineering* 190.42 (2001), pp. 5515–5528. ISSN: 0045-7825. DOI: https://doi.org/10.1016/S0045-7825(01)00180-3.

[36] G. R. Liu and Y. T. Gu. "A point interpolation method for two-dimensional solids". In: *International Journal for Numerical Methods in Engineering* 50.4 (2001), pp. 937–951. DOI: https://doi.org/10.1002/1097-0207(20010210)50:4<937::AID-NME62>3.0.CO;2-X.

[37] Gui-Rong Liu et al. "An extended Galerkin weak form and a point interpolation method with continuous strain field and superconvergence using triangular mesh". In: *Computational Mechanics* 43.5 (2009), pp. 651–673.

[38] X. Xu et al. "A point interpolation method with locally smoothed strain field (PIM-LS2) for mechanics problems using triangular mesh". In: *Finite Elements in Analysis and Design* 46.10 (2010), pp. 862–874. ISSN: 0168-874X. DOI: https://doi.org/10.1016/j.finel.2010.05.005.

[39] G.R. Liu and Y.T. Gu. "A matrix triangularization algorithm for the polynomial point interpolation method". In: *Computer Methods in Applied Mechanics and Engineering* 192.19 (2003), pp. 2269–2295. ISSN: 0045-7825. DOI: https://doi.org/10.1016/S0045-7825(03)00266-4.

[40] F. Cornacchia et al. "Solution for cross- and angle-ply laminated Kirchhoff nano plates in bending using strain gradient theory". In: *Composites Part B: Engineering* 173 (2019), p. 107006. ISSN: 1359-8368. DOI: https://doi.org/10.1016/j.compositesb.2019.107006.

[41] Bing-Bing Xu, Xiao-Wei Gao, and Miao Cui. "High precision simulation of thermal-mechanical problems in functionally graded materials by spectral element differential method". In: *Composite Structures* 270 (2021), p. 114084. ISSN: 0263-8223. DOI: https://doi.org/10.1016/j.compstruct.2021.114084.

[42] António JM Ferreira. *MATLAB codes for finite element analysis*. Springer, 2009.

[43] Paolo Maria Mariano and Patrizia Trovalusci. "Constitutive relations for elastic microcracked bodies: from a lattice model to a multifield continuum description". In: *International Journal of Damage Mechanics* 8.2 (1999), pp. 153–173.

[44] Lorenzo Leonetti et al. "Scale Effects in Orthotropic Composite Assemblies as Micropolar Continua: A Comparison between Weak- and Strong-Form Finite Element Solutions". In: *Materials* 12.758 (2019). ISSN: 1996-1944. DOI: 10.3390/ma12050758.

[45] Trovalusci, P. and Augusti, G. "A continuum model with microstructure for materials with flaws and inclusions". In: *J. Phys. IV France* 08.PR8 (1998), pp. 383–390. DOI: 10.1051/jp4:1998847. URL: https://doi.org/10.1051/jp4:1998847.

[46] Meral Tuna, Mesut Kirca, and Patrizia Trovalusci. "Deformation of atomic models and their equivalent continuum counterparts using Eringen's two-phase local/nonlocal model". In: *Mechanics Research Communications* 97 (2019), pp. 26–32. ISSN: 0093-6413. DOI: https://doi.org/10.1016/j.mechrescom.2019.04.004.

[47] Nicholas Fantuzzi, Patrizia Trovalusci, and Snehith Dharasura. "Mechanical behavior of anisotropic composite materials as micropolar continua". In: *Frontiers in Materials* 6 (2019), p. 59.

[48] Geminiano Mancusi et al. "Size effect and dynamic properties of 2D lattice materials". In: *Composites Part B: Engineering* 112 (2017), pp. 235–242. ISSN: 1359-8368. DOI: https://doi.org/10.1016/j.compositesb.2016.12.026.

[49] Ali Alizadeh et al. "A Modified Couple Stress-Based Model for the Nonlinear Vibrational Analysis of Nano-Disks Using Multiple Scales Method". In: *Journal of Applied and Computational Mechanics* (2021).

[50] R Luciano and J.R Willis. "Non-local constitutive response of a random laminate subjected to configuration-dependent body force". In: *Journal of the Mechanics and Physics of Solids* 49.2 (2001), pp. 431–444. ISSN: 0022-5096. DOI: https://doi.org/10.1016/S0022-5096(00)00031-4.

[51] Avey Mahmure et al. "Primary resonance of double-curved nanocomposite shells using nonlinear theory and multi-scales method: Modeling and analytical solution". In: *International Journal of Non-Linear Mechanics* 137 (2021), pp. 103–816. ISSN: 0020-7462. DOI: https://doi.org/10.1016/j.ijnonlinmec.2021.103816.

[52] M. Avey et al. "Nonlinear vibration of multilayer shell-type structural elements with double curvature consisting of CNT patterned layers within different theories". In: *Composite Structures* 275 (2021), p. 114401. ISSN: 0263-8223. DOI: https://doi.org/10.1016/j.compstruct.2021.114401.

[53] Ali Deniz et al. "Modeling and Solution of Large Amplitude Vibration Problem of Construction Elements Made of Nanocomposites Using Shear Deformation Theory". In: *Materials* 14.3843 (2021). ISSN: 1996-1944. DOI: 10.3390/ma14143843. URL: https://www.mdpi.com/1996-1944/14/14/3843.

[54] Francesco Cornacchia et al. "Tensile strength of the unbonded flexible pipes". In: *Composite Structures* 218 (2019), pp. 142–151. ISSN: 0263-8223. DOI: https://doi.org/10.1016/j.compstruct.2019.03.028.

[55] Marko Čanaija, Raffaele Barretta, and Francesco Marotti de Sciarra. "A gradient elasticity model of Bernoulli–Euler nanobeams in non-isothermal environments". In: *European Journal of Mechanics - A/Solids* 55 (2016), pp. 243–255. ISSN: 0997-7538. DOI: https://doi.org/10.1016/j.euromechsol.2015.09.008.

[56] R. Barretta, S. Ali Faghidian, and R. Luciano. "Longitudinal vibrations of nano-rods by stress-driven integral elasticity". In: *Mechanics of Advanced Materials and Structures* 26.15 (2019), pp. 1307–1315. DOI: 10.1080/15376494.2018.1432806.

[57] Hayri Metin Numanoğlu, Bekir Akgöz, and Ömer Civalek. "On dynamic analysis of nanorods". In: *International Journal of Engineering Science* 130 (2018), pp. 33–50. ISSN: 0020-7225. DOI: https://doi.org/10.1016/j.ijengsci.2018.05.001.

[58] Raffaele Barretta et al. "Functionally graded Timoshenko nanobeams: A novel nonlocal gradient formulation". In: *Composites Part B: Engineering* 100 (2016), pp. 208–219. ISSN: 1359-8368. DOI: https://doi.org/10.1016/j.compositesb.2016.05.052.

[59] Raffaele Barretta and Francesco Marotti de Sciarra. "A nonlocal model for carbon nanotubes under axial loads". In: *Advances in Materials Science and Engineering* 2013 (2013).

[60] Raffaele Barretta and Raimondo Luciano. "Analogies between Kirchhoff plates and functionally graded Saint-Venant beams under torsion". In: *Continuum Mechanics and Thermodynamics* 27.3 (2015), pp. 499–505.

[61] Raffaele Barretta and Raimondo Luciano. "Exact solutions of isotropic viscoelastic functionally graded Kirchhoff plates". In: *Composite Structures* 118 (2014), pp. 448–454. ISSN: 0263-8223. DOI: https://doi.org/10.1016/j.compstruct.2014.07.044.

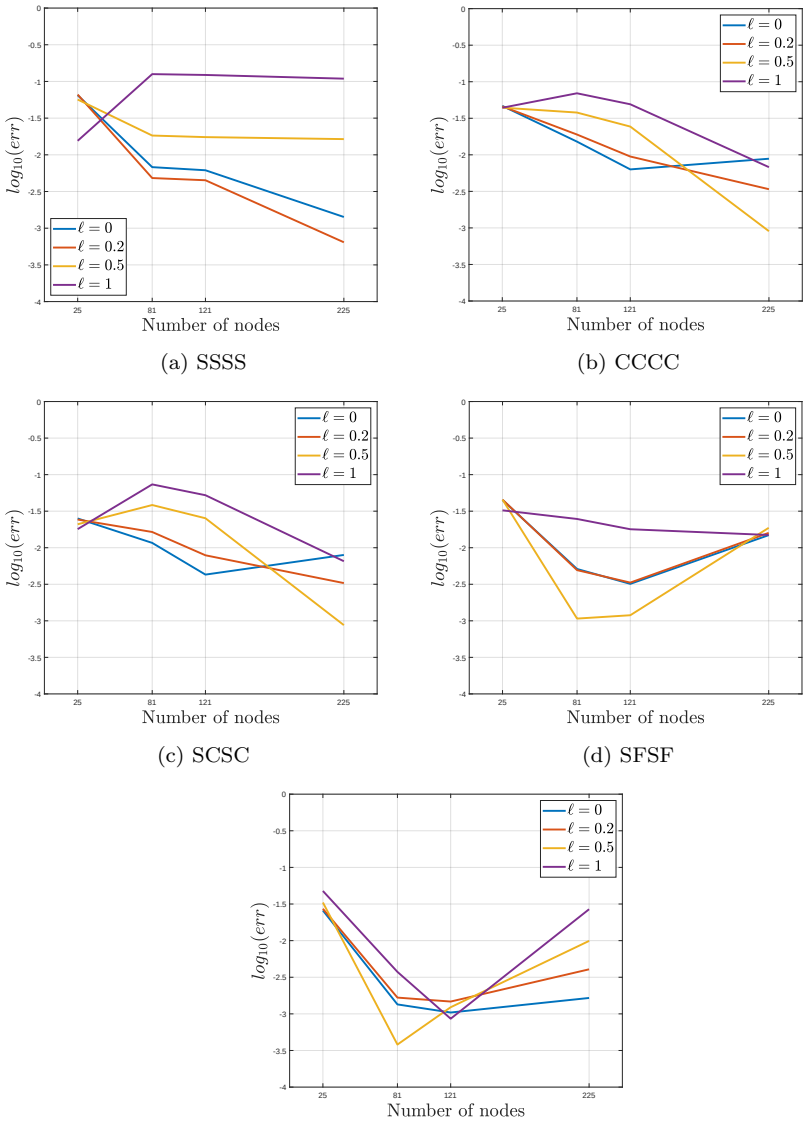

(a) SSSS

(b) CCCC

(c) SCSC

(d) SFSF

(e) SCSF

Figure 1: Convergence analysis for nanoplates with ratio $b/a = 0.5$.

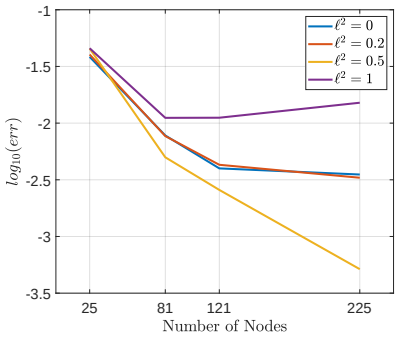

(a) SSSS

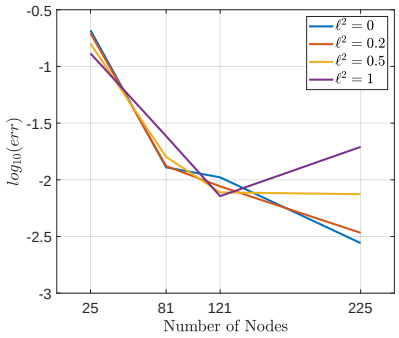

(b) CCCC

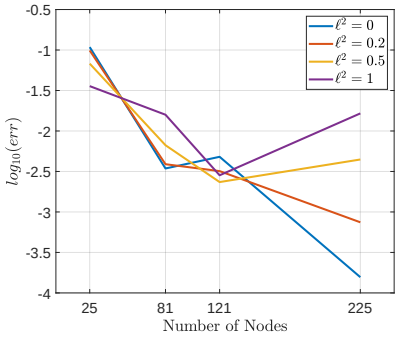

(c) SCSC

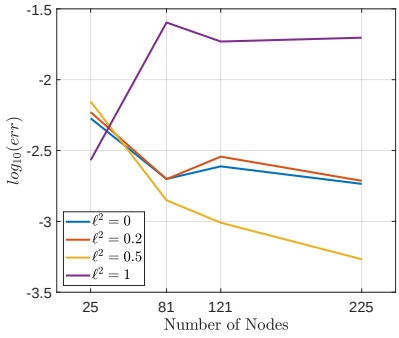

(d) SFSF

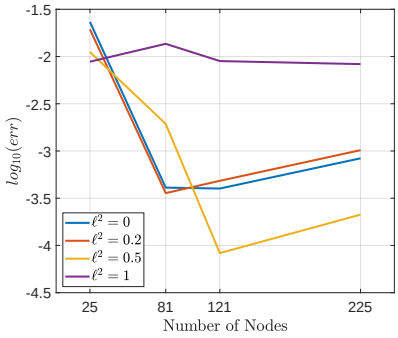

(e) SCSF

Figure 2: Convergence analysis for nanoplates with ratio $b/a = 1$.

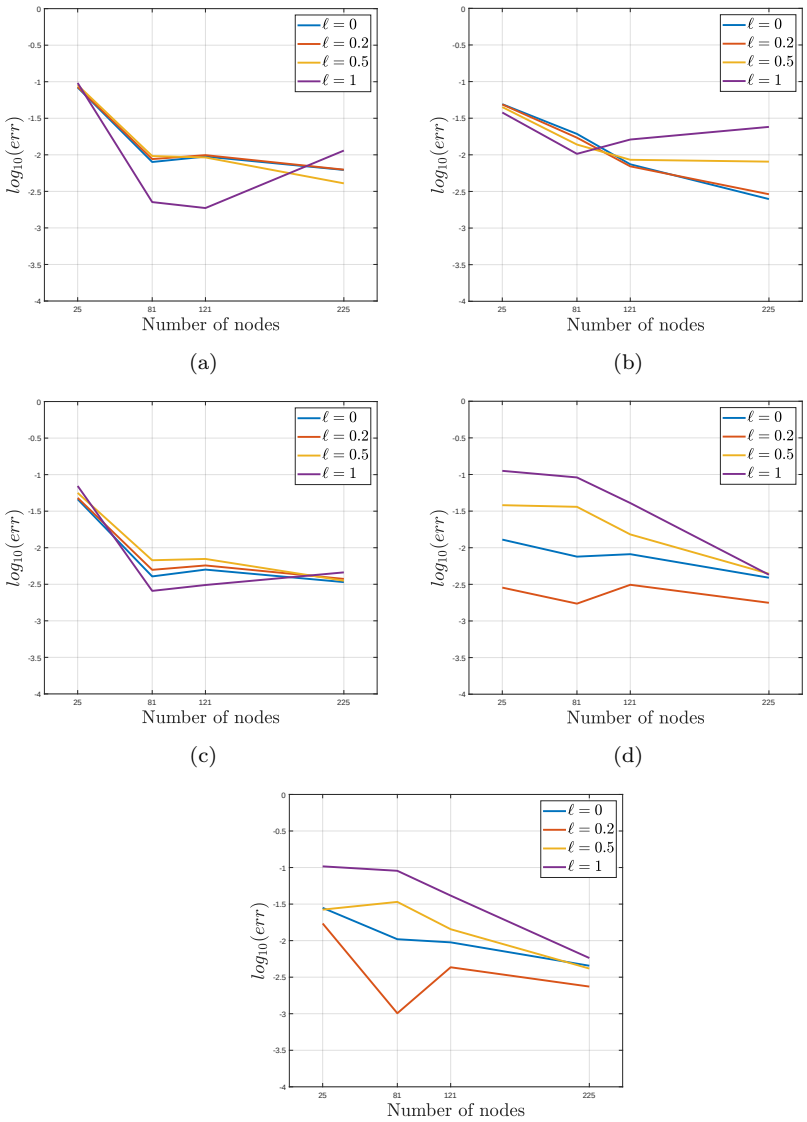

Figure 3: Convergence analysis for nanoplates with ratio $b/a = 2$.

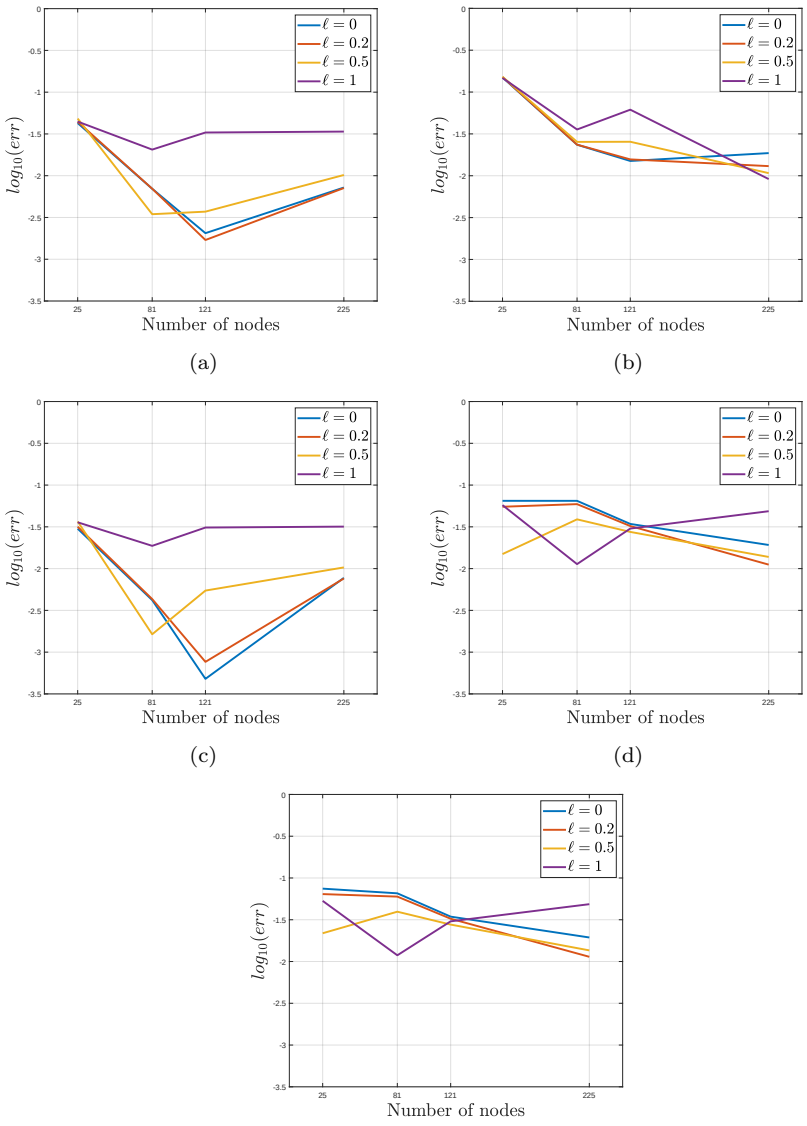

Figure 4: Convergence analysis for nanoplates with ratio $b/a = 3$.